ALTAY CONFERENCE PROCEEDINGS IN MATHEMATICS
1 (2025), No. 1, pp. 73-94
https://altayconfproceedings.com/

Research Article

Propagation of solitons and nonlinear behavior in nonlinear power law fibers

MUHAMMAD ABUBAKAR ISAH AND AHMAD MUHAMMAD*

ABSTRACT. This study investigates soliton propagation within the framework of nonlinear optics, specifically under the influence of a detuning parameter modeled by the complex GinzburgLandau equation (CGLE). Employing the φ^6-model expansion method, we derive a diverse set of analytical solutions, including trigonometric, hyperbolic, and rational function solutions. Notably, singular soliton solutions are obtained and shown to exhibit positive characteristics. The analysis is conducted in the context of nonlinear optical fibers governed by a power-law nonlinearity. The results contribute to a deeper understanding of the nonlinear dynamical behavior inherent in the CGLE and highlight the effectiveness of the applied method as a robust and efficient tool for obtaining reliable solutions to a wide class of nonlinear partial differential equations. To illustrate the physical features of the obtained solutions, several representative results are visualized through two-dimensional, three-dimensional, and contour plots.

Keywords: φ^6-model expansion approach, the complex Ginzburg–Landau equation, traveling wave solution, power law nonlinearity.

2020 Mathematics Subject Classification: 35Qxx, 35Exx.

1. INTRODUCTION

Optical solitons represent one of the most rapidly advancing areas of research in optoelectronics and nanoelectronics. A growing body of literature regularly reports new findings on this topic, reflecting its increasing significance. Various mathematical models have been developed to describe the propagation dynamics of solitons in optical fibers, including the nonlinear Schrödinger equation, the Schrödinger-Hirota equation, the Sasa-Satsuma equation, the Manakov equation, the Biswas-Milovic equation, and several others. Among these, the Complex GinzburgLandau Equation (CGLE) stands out as a particularly prominent model for capturing soliton behavior. Over the past few decades, numerous analytical and numerical methods have been devised to study the evolution of nonlinear systems across diverse physical domains-from fluid dynamics to optical wave propagation [20, 24, 8, 9, 22, 12, 18, 10, 25, 13, 5, 26, 14]. Analytical solitary wave solutions play a crucial role in understanding and analyzing long-distance signal transmission in optical communication systems, especially over transcontinental and trans-oceanic spans. Recent studies further underscore the importance of optical solitons in various branches of photonics, particularly in nonlinear optics and spectroscopy [23, 19, 21, 11, 6, 7].

In recent years, the Complex GinzburgLandau Equation (CGLE) with power-law nonlinearity has attracted significant attention from researchers. Mirzazadeh et al. [4] employed the

Received: 29.08.2025; Accepted: 07.10.2025; Published Online: 22.10.2025
*Corresponding author: Ahmad Muhammad; a.muhammad@qu.edu.qa
DOI: 10.64700/altay.21
Presented in *3rd International Conference: Constructive Mathematical Analysis*

semi-inverse variational principle to derive certain trivial solutions to the equation. Arnous, Ahmed H. et al. [2] applied the modified simple equation method to obtain bright and singular soliton solutions. Arshed [3] utilized the exp(-$\Phi(\xi)$)-expansion method and reported several distinct types of soliton solutions. Mirzazadeh, Mohammad et al. [28] adopted multiple integration schemes to extract a variety of soliton solutions, while Al-Ghafri [1] employed the Weierstrass elliptic function approach along with hyperbolic function solutions to obtain bright and singular solitons. In the present study, the CGLE with power-law nonlinearity is investigated using the recently developed φ^6-model expansion method [15, 17, 29, 27, 16]. This approach enables the recovery of optical solitary wave solutions, further demonstrating the methods effectiveness in handling complex nonlinear systems.

The paper is structured as follows. Section 2 outlines the mathematical formulation and theoretical analysis of the model. In Section 3, we provide a detailed description of the φ^6-model expansion method, highlighting its methodology and underlying principles. Section 4 applies this approach to the complex GinzburgLandau Equation (CGLE) with power-law nonlinearity, successfully deriving a variety of novel traveling wave solutions. The physical characteristics of these solutions are visualized through three-dimensional and density plots, and a brief discussion on the dynamical behavior of the obtained solitons is also presented. Finally, Section 5 offers concluding remarks and highlights the broader implications of the results.

2. Mathematical analysis of the model

In this study, we adopt the dimensionless formulation of the (GCLE) as presented in [2, 27], which serves as the basis for our subsequent analysis

$$iq_t + aq_{xx} + bF(|q|^2)q = \frac{1}{|q|^2 q^\star}\left[\alpha |q|^2 (|q|^2)_{xx} - \beta \left\{(|q|^2)_x\right\}^2\right] + \gamma q. \tag{2.1}$$

Here, q denotes a complex-valued function representing the wave profile observed in various physical contexts, including nonlinear optics and plasma physics. The variable x corresponds to the non-dimensional spatial coordinate along the fiber, and t denotes the dimensionless time. The parameters a, b, α, β and γ are real-valued constants, where a and b are associated with the Group Velocity Dispersion (GVD) and the nonlinear coefficient, respectively. The coefficients α, β and γ arise from perturbative effects, particularly detuning.

In Eq. (2.1), F denotes a smooth, real-valued algebraic function, and the term $F(|q|^2)q$ is assumed to be k-times continuously differentiable. These smoothness and differentiability requirements ensure the well-posedness of the model and facilitate the application of analytical techniques to obtain exact or approximate solutions, implying that

$$F(|q|^2)q \in \cup_{n,m=1}^{\infty} C^k\left((-m,m)\times(-n,n)\,;R^2\right). \tag{2.2}$$

By setting up

$$\alpha = 2\beta. \tag{2.3}$$

Eq. (2.1) turns to

$$iq_t + aq_{xx} + bF(|q|^2)q = \frac{\beta}{|q|^2 q^\star}\left[2 |q|^2 (|q|^2)_{xx} - \left\{(|q|^2)_x\right\}^2\right] + \gamma q. \tag{2.4}$$

The solution of Eq. (2.1) proceeds via the standard decomposition into amplitude and phase components

$$q\,(x,t) = P(\psi)e^{i(-kx+wt+\theta)} \tag{2.5}$$

and the wave variable ψ is expressed as

$$\psi = \lambda\,(x - vt)\,. \tag{2.6}$$

Here, the function P characterizes the pulse shape, while v denotes the solitons velocity. In the phase factor, k corresponds to the soliton frequency, ω to the soliton wave number, and θ to the phase constant. Inserting the amplitudephase decomposition into Eq. (2.4) and separating the result into real and imaginary parts yields the following pair of equations:

$$-\left(ak^2 + \gamma + \omega\right) P + bF\left(P^2\right) P + \lambda^2\,(a - 4\beta)\, P^{''} = 0 \tag{2.7}$$

and

$$v = -2ka. \tag{2.8}$$

In the part 4 of this paper, Eq. (2.7) will be examined using power law of nonlinearity.

3. Description of the method

Based on the work in [5, 15, 17, 29, 27, 16], the essential steps of the recently proposed φ^6-model expansion technique are given below:

Step-1: We consider the Nonlinear Evolution Equation (NLEE) given for $q = q(x,t)$ below

$$H(q, q_x, q_t, q_{xx}, q_{xt}, ...) = 0. \tag{3.9}$$

Here, H denotes a polynomial in $q(x,t)$ and its highest-order partial derivatives, which also includes the nonlinear components.

Step-2: Utilizing the wave transformation

$$q(x,t) = q(\psi), \quad \psi = x - vt. \tag{3.10}$$

Here, v represents the wave speed, allowing Eq. (3.9) to be rewritten as the following nonlinear ordinary differential equation.

$$\Omega(q, q^{'}, qq^{'}, q^{''}, ...) = 0, \tag{3.11}$$

where primes denote derivatives with respect to ψ.

Step-3: Let us suppose that Eq. (3.11) admits a formal solution:

$$q\,(\psi) = \sum_{i=0}^{2N} \alpha_i U^i(\psi), \tag{3.12}$$

where $\alpha_i (i = 0, 1, 2, \ldots, N)$ represent undetermined constants, N is determined via the balancing method, and $U(\psi)$ is a solution of the auxiliary Nonlinear Ordinary Differential Equation (NLODE);

$$U'^2(\psi) = h_0 + h_2U^2(\psi) + h_4U^4(\psi) + h_6U^6(\psi), \tag{3.13}$$
$$U^{''}(\psi) = h^2U(\psi) + 2h_4U^3(\psi) + 3h_6U^5(\psi),$$

here, the real constants $h_i($ with $i = 0, 2, 4, 6)$ will be identified in subsequent steps.

Step-4: The solution to Eq. (3.13) is commonly known to be;

$$U(\psi) = \frac{P(\psi)}{\sqrt{fP^2(\psi) + g}}, \tag{3.14}$$

provided that $0 < fP^2(\psi) + g$ and $P(\psi)$ is the Jacobi elliptic equation solution

$$P'^2(\psi) = l_0 + l_2P^2(\psi) + l_4P^4(\psi), \tag{3.15}$$

here, the unknown constants l_i (with $i = 0, 2, 4$) are to be determined, while f and g are expressed as

$$f = \frac{h_4(l_2 - h_2)}{(l_2 - h_2)^2 + 3l_0 l_4 - 2l_2(l_2 - h_2)},$$
$$g = \frac{3l_0 h_4}{(l_2 - h_2)^2 + 3l_0 l_4 - 2l_2(l_2 - h_2)}, \tag{3.16}$$

under the restriction condition

$$h_4^2(l_2 - h_2)[9l_0 l_4 - (l_2 - h_2)(2l_2 + h_2)] + 3h_6[-l_2^2 + h_2^2 + 3l_0 l_4]^2 = 0. \tag{3.17}$$

Step-5: As discussed in [5], the Jacobi elliptic function solutions of Eq. (3.15) are well-established for values of ρ in the interval $0 < \rho < 1$. By substituting these solutions, along with Eq. (3.14), into the solution ansatz given in Eq. (3.12), we obtain exact analytical solutions to Eq. (3.9).

Function	$\rho \to 1$	$\rho \to 0$	Function	$\rho \to 1$	$\rho \to 0$
$sn(\psi, \rho)$	$tanh(\psi)$	$sin(\psi)$	$ds(\psi, \rho)$	$csch(\psi)$	$csc(\psi)$
$cn(\psi, \rho)$	$sech(\psi)$	$cos(\psi)$	$sc(\psi, \rho)$	$sinh(\psi)$	$tan(\psi)$
$dn(\psi, \rho)$	$sech(\psi)$	1	$sd(\psi, \rho)$	$sinh(\psi)$	$sin(\psi)$
$ns(\psi, \rho)$	$coth(\psi)$	$csc(\psi)$	$nc(\psi, \rho)$	$cosh(\psi)$	$sec(\psi)$
$cs(\psi, \rho)$	$csch(\psi)$	$cot(\psi)$	$cd(\psi, \rho)$	1	$cos(\psi)$

TABLE 1. Jacobi elliptic functions

4. IMPLEMENTATION OF THE φ^6-MODEL EXPANSION METHOD

Power-law nonlinearity arises naturally in a variety of physical systems and is particularly prominent in materials such as semiconductors, doped glasses, and photorefractive media, where the nonlinear response of the refractive index depends on the intensity of the optical field in a non-quadratic manner. This type of nonlinearity is widely regarded as a natural generalization of the well-known Kerr law (which corresponds to the case $n = 1$), offering a more flexible and physically realistic framework for modeling nonlinear optical phenomena. In this context, the nonlinear function takes the form $F(u) = u^n$, allowing for a broader range of nonlinear behaviors depending on the value of the exponent n. Under this assumption, Eq. (2.4) reduces to a generalized version of the Complex GinzburgLandau Equation (CGLE) that accommodates higher or lowernorder nonlinearities, making it applicable to a wider class of optical media beyond those governed by cubic nonlinearities. This generalization is not only mathematically significant but also physically meaningful, as it enables the modeling of soliton propagation in engineered materials where the nonlinear response deviates from standard Kerr-type behavior [4, 2, 3, 28]. The parameter n thus plays a critical role in tuning the strength and nature of the nonlinearity, influencing the existence, stability, and dynamical properties of the resulting soliton solutions. In this case, Eq. (2.4) reduces to

$$iq_t + (b\,|q|^{2n})q + aq_{xx} = \frac{\beta}{|q|^2\, q^\star}\left[2\,|q|^2\,(|q|^2)_{xx} - \left\{(|q|^2)_x\right\}^2\right] + \gamma q, \tag{4.18}$$

and Eq. (2.7) is transformed

$$-\left(ak^2 + \gamma + \omega\right)P + bP^{2n+1} + \lambda^2\,(a - 4\beta)\,P^{''} = 0. \tag{4.19}$$

Here in Eq. (4.18) the parameter n dictates the power law nonlinearity. For stability issues, it is necessary to have $0 < n < 2$, and in particular $n \neq 2$, to avoid self-focusing singularity.

Setting

$$P = p^{\frac{1}{n}},$$

Eq. (4.19) transform to

$$-n^2\left(ak^2+\gamma+\omega\right)p^2+n^2bp^4+\lambda^2\left(a-4\beta\right)\left[\left(1-n\right)\left(p^{'}\right)^2+npp^{''}\right]=0. \tag{4.20}$$

In Eq. (4.20), we get $N = 1$ by balancing $pp^{''}$ with P^4, we obtain the following by substituting $N = 1$ in Eq. (3.12).

$$P(\psi) = \alpha_0 + \alpha_1 U(\psi) + \alpha_2 U^2(\psi), \tag{4.21}$$

where α_0, α_1 and α_2 are constants to be determined.

By substituting the solution ansatz given in Eq. (4.21) and the auxiliary ordinary differential equation Eq. (3.13) into Eq. (4.19), and collecting terms of each power of $U^i(\psi)$, $i = 0, 1, \ldots, 8$, we obtain a system of algebraic equations by setting the coefficients of like powers to zero.

$$\begin{aligned}
U^0(\psi) &: -n^2\left(ak^2+\gamma+\omega\right)\alpha_0^2+bn^2\alpha_0^4\\
&\quad -\lambda^2\left(-1+n\right)\left(a-4\beta\right)h_0\alpha_1^2+2\lambda^2n\left(a-4\beta\right)h_0\alpha_0\alpha_2=0,\\
U^1(\psi) &: -n\alpha_0\alpha_1\left(2n\left(ak^2+\gamma+\omega\right)-\lambda^2\left(a-4\beta\right)h_2\right)\\
&\quad +4bn^2\alpha_0^3\alpha_1-2\lambda^2\alpha_1\left(-2+n\right)\left(a-4\beta\right)h_0\alpha_2=0,\\
U^2(\psi) &: -\left(-\lambda^2\left(a-4\beta\right)h_2+n^2\left(ak^2+\gamma+\omega-6b\alpha_0^2\right)\right)\alpha_1^2\\
&\quad -2n\alpha_0\left(-2\lambda^2\left(a-4\beta\right)h_2+n\left(ak^2+\gamma+\omega-2b\alpha_0^2\right)\right)\alpha_2\\
&\quad -2\lambda^2\left(-2+n\right)\left(a-4\beta\right)h_0\alpha_2^2=0,\\
U^3(\psi) &: \alpha_1\left(2\lambda^2n\left(a-4\beta\right)h_4\alpha_0+4bn^2\alpha_0\alpha_1^2\right)\\
&\quad +\alpha_1\alpha_2\left(\lambda^2\left(4+n\right)\left(a-4\beta\right)h_2-2n^2\left(ak^2+\gamma+\omega-6b\alpha_0^2\right)\right)=0,\\
U^4(\psi) &: bn^2\alpha_1^4+12bn^2\alpha_0\alpha_1^2\alpha_2-\left(-4\lambda^2\left(a-4\beta\right)h_2+n^2\left(ak^2+\gamma+\omega-6b\alpha_0^2\right)\right)\alpha_2^2\\
&\quad +\lambda^2\left(a-4\beta\right)h_4\left(\left(1+n\right)\alpha_1^2+6n\alpha_0\alpha_2\right)=0,\\
U^5(\psi) &: 3\lambda^2n\left(a-4\beta\right)h_6\alpha_0\alpha_1+4\alpha_1\alpha_2\left(\lambda^2\left(1+n\right)\left(a-4\beta\right)h_4+bn^2\left(\alpha_1^2+3\alpha_0\alpha_2\right)\right)=0,\\
U^6(\psi) &: \lambda^2\left(a-4\beta\right)h_6\left(\left(1+2n\right)\alpha_1^2+8n\alpha_0\alpha_2\right)\\
&\quad +2\alpha_2^2\left[\lambda^2\left(2+n\right)\left(a-4\beta\right)h_4+bn^2\left(3\alpha_1^2+2\alpha_0\alpha_2\right)\right]=0,\\
U^7(\psi) &: \alpha_1\alpha_2\left[\lambda^2\left(4+7n\right)\left(a-4\beta\right)h_6+4bn^2\alpha_2^2\right]=0,\\
U^8(\psi) &: 4\lambda^2\left(1+n\right)\left(a-4\beta\right)h_6\alpha_2^2+bn^2\alpha_2^4=0.
\end{aligned} \tag{4.22}$$

We get the following result after solving the resulting system:

$$\begin{aligned}
&\alpha_0=0,\quad \alpha_1=\frac{\lambda\sqrt{1+n}\sqrt{\left(-a+4\beta\right)h_4}}{\sqrt{bn}},\quad h_2=\frac{n^2\left(ak^2+\gamma+\omega\right)}{\lambda^2\left(a-4\beta\right)},\\
&\alpha_2=0,\quad h_0=0,\quad h_4=h_4,\qquad h_6=0.
\end{aligned} \tag{4.23}$$

In view of Eqs. (3.14), (4.21) and (4.23) along with the Jacobi elliptic functions in the above table, we obtain the following exact solutions of Eq. (4.18)

1. If $l_0 = 1$, $l_2 = -(1+\rho^2)$, $l_4 = \rho^2$, $0 < \rho < 1$, then $P(\psi) = sn(\psi, \rho)$ or $P(\psi) = cd(\psi, \rho)$, and we have

$$q_{1,1}\left(x,t\right)=\left[\frac{\lambda\sqrt{1+n}\sqrt{\left(-a+4\beta\right)h_4}}{\sqrt{b}n}\left(\frac{sn(\psi,\rho)}{\sqrt{f\left(sn(\psi,\rho)\right)^2+g}}\right)\right]^{\frac{1}{n}}e^{i(-kx+wt+\theta)}, \tag{4.24}$$

or

$$q_{1,2}\left(x,t\right)=\left[\frac{\lambda\sqrt{1+n}\sqrt{\left(-a+4\beta\right)h_4}}{\sqrt{b}n}\left(\frac{cd(\psi,\rho)}{\sqrt{f\left(cd(\psi,\rho)\right)^2+g}}\right)\right]^{\frac{1}{n}}e^{i(-kx+wt+\theta)}, \tag{4.25}$$

such that $0<b,\ \psi=\lambda\left(x-vt\right)$, and f and g in Eq. (3.16) are given by

$$f=\frac{(1+\rho^2+h_2)h_4}{1-\rho^2+\rho^4-h_2^2},$$
$$g=\frac{-3h_4}{1-\rho^2+\rho^4-h_2^2},$$

under the restriction condition

$$-h_4^2\left(-1-\rho^2-h_2\right)\left(-1+2\rho^2-h_2\right)\left(-2+\rho^2+h_2\right)=0.$$

If $\rho\to 1$, then the dark soliton is obtained

$$q_{1,3}\left(x,t\right)=\left[\frac{\lambda\sqrt{1+n}\sqrt{\left(-a+4\beta\right)h_4}}{\sqrt{b}n}\left(\frac{\tanh(\psi)}{\sqrt{\frac{h_4(3-(2+h_2)\tanh^2(\psi))}{-1+h_2^2}}}\right)\right]^{\frac{1}{n}}e^{i(-kx+wt+\theta)}. \tag{4.26}$$

Here in Eq. (4.26), the parameter n dictates the power law nonlinearity. For stability issues, it is necessary to have $0<n<2$, and in particular $n\neq 2$, to avoid self-focusing singularity. Setting $n=1$, results in generelization of kerr law nonlinearity, the dark soliton is now obtained as

$$q_{1,3}\left(x,t\right)=\frac{i\sqrt{2}\lambda\sqrt{a-4\beta}e^{i(-kx+\theta+tw)}\tanh(\lambda(2akt+x))}{\sqrt{b}}, \tag{4.27}$$

such that

$$h_4^2\left(-2-h_2\right)\left[\left(-1+h_2\right)^2\right]=0.$$

Figure 1 illustrates the dark soliton solution $q_{1,3}(x,t)$ derived in Eq.(4.27) for the limiting case $\rho=1$, where the Jacobi elliptic function reduces to a $\tanh(x)$ profile. The modulus plot (a) and contour plot (b) show the characteristic intensity dip that propagates on a continuous background, confirming the presence of a moving dark soliton. The real and imaginary parts in (c) exhibit a localized π-phase shift, which is a hallmark of dark solitons in defocusing media. In the context of nonlinear fiber optics, such dark solitons arise in fibers exhibiting normal dispersion and self-defocusing nonlinearity, particularly in photonic crystal fibers or fiber Bragg gratings. These solitons are valuable for optical switching, intensity dips for logic gates, and phase-sensitive modulation schemes. Their robustness under power-law nonlinearity suggests potential for advanced pulse shaping and energy channeling in nonlinear waveguides with engineered refractive index profiles. These solutions are physically relevant to nonlinear optical fibers with power-law refractive index profiles, where such localized dips may represent energy voids in high-intensity beam propagation or be employed for pulse modulation and switching.

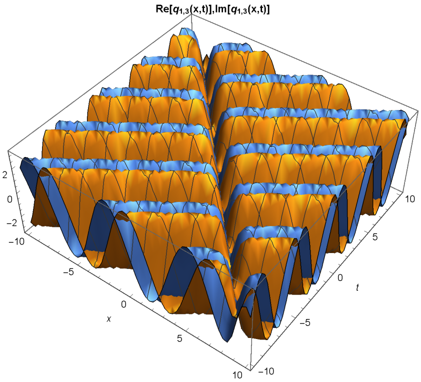

(A) $|q_{1,3}|$

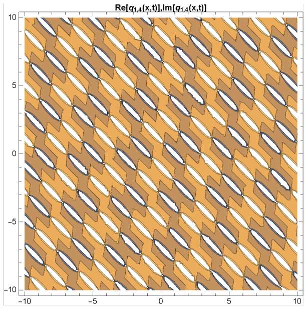

(B) $|q_{1,3}|$

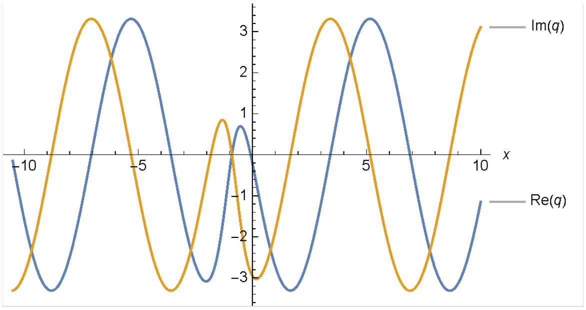

(C) $|q_{1,3}|$

FIGURE 1. The numerical simulations corresponding to $|q_{1,3}|$ given by Eq. (4.27), for $\rho = 1$; (a) is the 3D graphic, (b) is the 2D-contour graphic while (c) is the 3D graphic for $k = 0.9, \theta = 0.2, \omega = 1.3, a = 0.5, b = 0.7, \lambda = 1.6, \beta = 0.5$.

If $\rho \to 0$, then the periodic solution is obtained

$$q_{1,4}(x,t) = \left[\frac{\lambda\sqrt{1+n}\sqrt{(-a+4\beta)\,h_4}}{\sqrt{bn}} \left(\frac{\sin(\psi)}{\sqrt{\frac{h_4(3-(1+h_2)\sin^2(\psi))}{-1+h_2^2}}} \right) \right]^{\frac{1}{n}} e^{i(-kx+wt+\theta)}, \tag{4.28}$$

such that

$$h_4^2\,(-1-h_2)\,[(-2+h_2)\,(1+h_2)] = 0.$$

Figure 2 numerically validates the periodic solution $q_{1,4}(x,t)$ Eq. (4.28) for $\rho = 0$, where the Jacobi elliptic function reduces to a sinusoidal profile. The $3D$ plot (a) and contour (b) demonstrate coherent wave propagation with velocity $v = -1$, while the amplitude modulation reflects the nonlinear constraint $h_2 = 2$. Such periodic states are observable in dispersion-managed fibers under pump-driven nonlinearities, offering potential for frequency comb generation or all-optical signal processing. The parameter sensitivity in (c) emphasizes the need for precise control in experimental realizations.

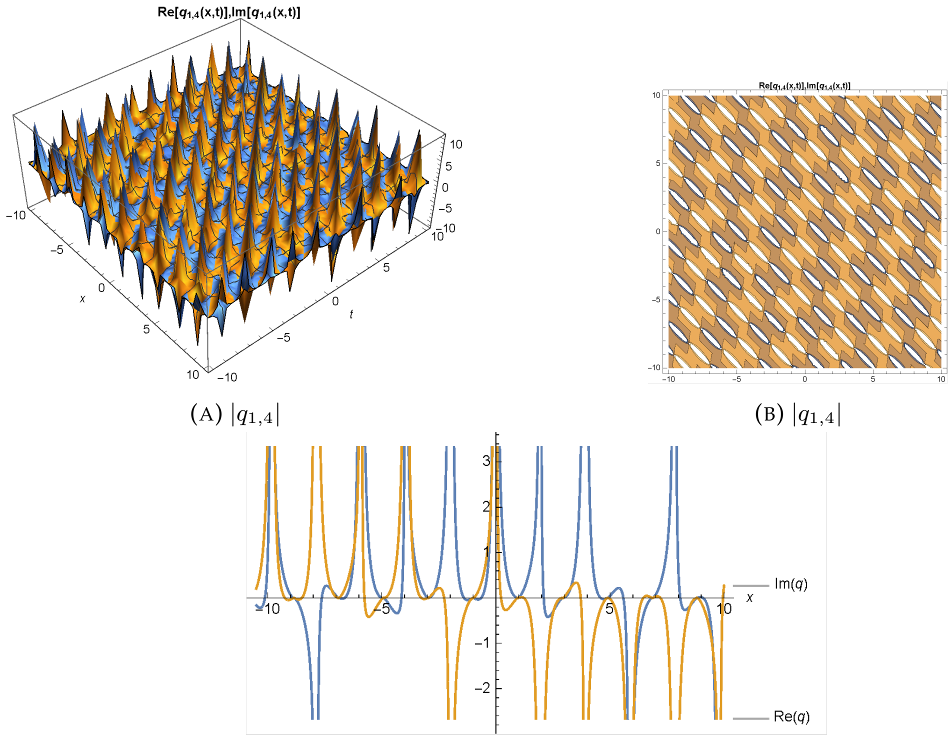

(A) $|q_{1,4}|$ (B) $|q_{1,4}|$

(C) $|q_{1,4}|$

FIGURE 2. The numerical simulations corresponding to $|q_{1,4}|$ given by Eq. (4.28), for $\rho = 0$; (a) is the 3D graphic, (b) is the 2D-contour graphic while (c) is the 3D graphic for $k = 1.8, \theta = 2, \omega = 0.2, v = -1, \gamma = -1.6, \beta = 0.8, a = -0.4, n = 0.7, \lambda = -1.6, h_4 = 2, c = 1.2, \alpha_1 = 1, h_2 = 2$.

2. If $l_0 = 1-\rho^2$, $l_2 = 2\rho^2 - 1$, $l_4 = -\rho^2$, $0 < \rho < 1$, then $P(\psi) = cn(\psi, \rho)$ therefore

$$q_2(x,t) = \left[\frac{\lambda\sqrt{1+n}\sqrt{(-a+4\beta)\,h_4}}{\sqrt{b}n} \left(\frac{cn(\psi,\rho)}{\sqrt{f\,(cn(\psi,\rho))^2+g}} \right) \right]^{\frac{1}{n}} e^{i(-kx+wt+\theta)}, \tag{4.29}$$

where f and g are determined by

$$f = -\frac{(-1+2\rho^2-h_2)h_4}{1-\rho^2+\rho^4-h_2^2},$$
$$g = \frac{3\left(-1+\rho^2\right)h_4}{1-\rho^2+\rho^4-h_2^2},$$

under the constraint condition

$$h_4^2\left(-1+2\rho^2-h_2\right)\left[\left(-2+\rho^2+h_2\right)\left(1+\rho^2+h_2\right)\right] = 0.$$

If $\rho \to 1$, then the bright soliton is retrieved

$$q_{2,1}(x,t) = \left[\frac{\lambda\sqrt{1+n}\sqrt{(-a+4\beta)\,h_4}}{\sqrt{bn}}\left(\frac{sech(\psi)}{\sqrt{\frac{-h_4 sech^2(\psi)}{1+h_2}}}\right)\right]^{\frac{1}{n}} e^{i(-kx+wt+\theta)} \tag{4.30}$$

provided that

$$h_4^2\,(1-h_2)\left[h_2^2+h_2-2\right]=0.$$

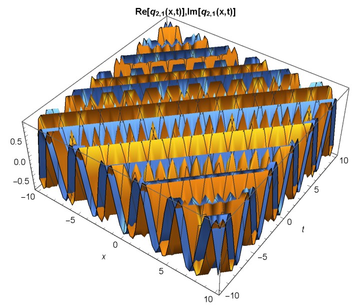

(A) $|q_{2,1}|$

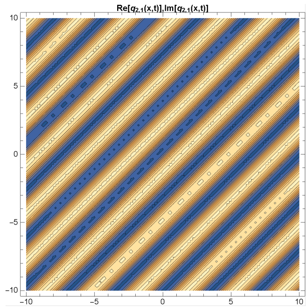

(B) $|q_{2,1}|$

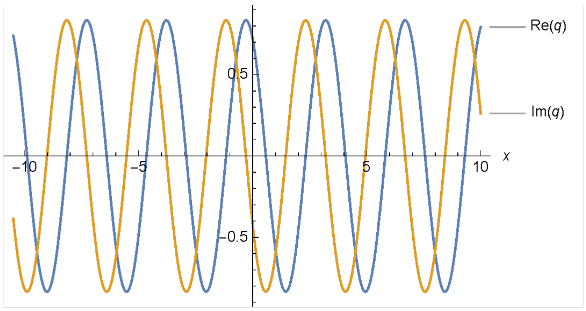

(C) $|q_{2,1}|$

FIGURE 3. The numerical simulations corresponding to $|q_{2,1}|$ given by Eq. (4.30), for $\rho = 1$; (a) is the 3D graphic , (b) is the 2D-contour graphic while (c) is the 3D graphic for $k = 1.8, \theta = 5, \omega = 1.8, v = 1, \gamma = 1, \beta = 0.8, a = 1, n = 1.5, \lambda = 1.6, h_4 = -2, c = 1.2, \alpha_1 = 1.078, h_2 = -2$.

Figure 3 numerically validates the bright soliton solution $q_{2,1}$ Eq. (4.30) for $\rho = 1$, where the Jacobi elliptic function reduces to $\mathrm{sech}(\psi)\,\mathrm{sech}(\psi)$. The 3D plot (a) and contour (b) demonstrate the solitons stable propagation, with the constraint $h_2 = -2$ ensuring a physical amplitude. Panel (c) reveals how parameter choices (e.g., $h_4 = -2$) tune the pulse shape critical for designing soliton-based fiber-optic systems. Such solutions are experimentally achievable in fibers with anomalous dispersion ($a < 4$) and power levels balancing nonlinearity and dispersion.

If $\rho \to 0$, then the periodic solution is obtained

$$q_{2,2}(x,t) = \left[\frac{\lambda\sqrt{1+n}\sqrt{(-a+4\beta)\,h_4}}{\sqrt{bn}}\left(\frac{\cos(\psi)}{\sqrt{\frac{-h_4(-3+(1+h_2)\cos^2(\psi))}{-1+h_2^2}}}\right)\right]^{\frac{1}{n}} e^{i(-kx+wt+\theta)}, \tag{4.31}$$

such that

$$h_4^2\left(-1-h_2\right)\left[\left(-2+h_2\right)\left(1+h_2\right)\right]=0.$$

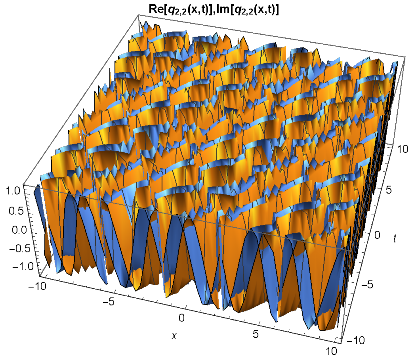

(A) $|q_{2,2}|$

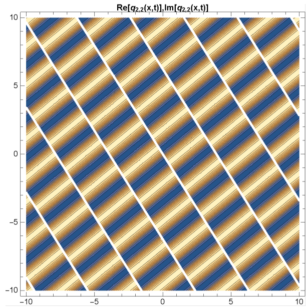

(B) $|q_{2,2}|$

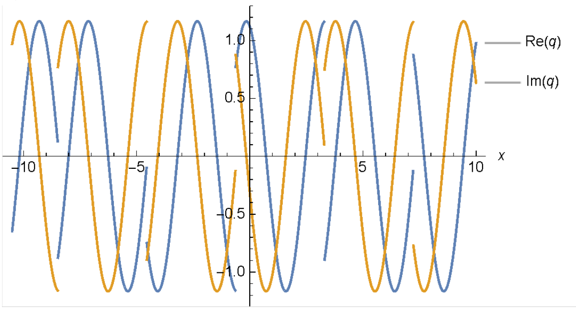

(C) $|q_{2,2}|$

FIGURE 4. The numerical simulations corresponding to $|q_{2,2}|$ given by Eq. (4.31), for $\rho = 0$; (a) is the 3D graphic, (b) is the 2D-contour graphic while (c) is the 3D graphic for $k = 1.8, \theta = 5, \omega = 2.2, v = -0.63, \gamma = 1, \beta = 0.8, a = 1, n = 1.32, \lambda = 0.8, h_4 = 2, c = 1.2, \alpha_1 = 1, h_2 = 2$.

Figure 4 numerically validates the periodic solution $q_{2,2}$ Eq. (4.31) for $\rho = 0$, where the profile reduces to a $\cos(\psi)$ wave. The 3D plot (a) and contour (b) demonstrate coherent propagation with velocity $v = -0.63$, while the amplitude modulation in (c) reflects the nonlinear constraint $h_2 = 2$. Such solutions model stimulated Brillouin scattering in fibers or optical lattice vibrations in waveguide arrays, with nodes/antinodes tunable via h_4 and λ.

3. If $l_0 = \rho^2 - 1, l_2 = 2 - \rho^2, l_4 = -1, 0 < \rho < 1$, then $P(\psi) = dn(\psi, \rho)$ which gives

$$q_3\left(x,t\right)=\left[\frac{\lambda\sqrt{1+n}\sqrt{\left(-a+4\beta\right)h_4}}{\sqrt{b}n}\left(\frac{dn(\psi,\rho)}{\sqrt{f\left(dn(\psi,\rho)\right)^2+g}}\right)\right]^{\frac{1}{n}}e^{i(-kx+wt+\theta)}, \tag{4.32}$$

where f and g are determined by

$$f = \frac{(-2+\rho^2+h_2)h_4}{1-\rho^2+\rho^4-h_2^2},$$
$$g = \frac{-3\left(-1+\rho^2\right)h_4}{1-\rho^2+\rho^4-h_2^2},$$

under the restriction condition

$$h_4^2\left(2-\rho^2-h_2\right)\left[-\left(-1+2\rho^2+h_2\right)\left(1+\rho^2+h_2\right)\right]=0.$$

If $\rho \to 1$, then the singular soliton solution is obtained

$$q_{3,1}(x,t) = \left[\frac{\lambda\sqrt{1+n}\sqrt{(-a+4\beta)h_4}}{\sqrt{b}n}\left(\frac{sech(\psi)}{\sqrt{\frac{-h_4 sech^2(\psi)}{1+h_2}}}\right)\right]^{\frac{1}{n}} e^{i(-kx+wt+\theta)}, \tag{4.33}$$

provided that

$$h_4^2\left(1-h_2\right)\left[-2+h_2+h_2^2\right]=0.$$

If $\rho \to 0$, then the rational solution is obtained

$$q_{3,2}(x,t) = \left[\frac{\lambda\sqrt{1+n}\sqrt{(-a+4\beta)h_4}}{\sqrt{b}n}\left(\frac{1}{\sqrt{\frac{h_4}{1-h_2}}}\right)\right]^{\frac{1}{n}} e^{i(-kx+wt+\theta)}, \tag{4.34}$$

such that

$$h_4^2\left(2-h_2\right)\left[\left(1+h_2\right)^2\right]=0.$$

4. If $l_0=\rho^2$, $l_2=-\left(1+\rho^2\right)$, $l_4=1, 0<\rho<1$, then $P(\psi)=ns(\psi,\rho)$ or $P(\psi)=dc(\psi,\rho)$ then

$$q_{4,1}(x,t) = \left[\frac{\lambda\sqrt{1+n}\sqrt{(-a+4\beta)h_4}}{\sqrt{b}n}\left(\frac{ns(\psi,\rho)}{\sqrt{f\left(ns(\psi,\rho)\right)^2+g}}\right)\right]^{\frac{1}{n}} e^{i(-kx+wt+\theta)}, \tag{4.35}$$

or

$$q_{4,2}(x,t) = \left[\frac{\lambda\sqrt{1+n}\sqrt{(-a+4\beta)h_4}}{\sqrt{b}n}\left(\frac{dc(\psi,\rho)}{\sqrt{f\left(dc(\psi,\rho)\right)^2+g}}\right)\right]^{\frac{1}{n}} e^{i(-kx+wt+\theta)}, \tag{4.36}$$

where f and g are given by

$$f = \frac{(1+\rho^2+h_2)h_4}{1-\rho^2+\rho^4-h_2^2},$$
$$g = \frac{-3\rho^2 h_4}{1-\rho^2+\rho^4-h_2^2},$$

under the constraint condition

$$h_4^2\left(-1-\rho^2-h_2\right)\left[-\left(-1+2\rho^2-h_2\right)\left(-2+\rho^2+h_2\right)\right]=0.$$

If $\rho \to 1$, then the dark singular solution is obtained

$$q_{4,3}(x,t) = \left[\frac{\lambda\sqrt{1+n}\sqrt{(-a+4\beta)h_4}}{\sqrt{b}n}\left(\frac{\coth(\psi)}{\sqrt{\frac{(-1+h_2+(2+h_2)\text{csch}^2(\psi))h_4}{1-h_2^2}}}\right)\right]^{\frac{1}{n}} e^{i(-kx+wt+\theta)} \tag{4.37}$$

such that

$$h_4^2\left(-2-h_2\right)\left[\left(-1+h_2\right)^2\right]=0.$$

If $\rho\to 0$, then the periodic solution is obtained

$$q_{4,4}\left(x,t\right)=\left[\frac{\lambda\sqrt{1+n}\sqrt{\left(-a+4\beta\right)h_4}}{\sqrt{b}n}\left(\frac{\csc(\psi)}{\sqrt{\frac{-\csc^2(\psi)h_4}{-1+h_2}}}\right)\right]^{\frac{1}{n}}e^{i(-kx+wt+\theta)}, \tag{4.38}$$

such that

$$h_4^2\left(-1-h_2\right)\left[\left(-2+h_2\right)\left(1+h_2\right)\right]=0.$$

5. If $l_0=-\rho^2$, $l_2=2\rho^2-1$, $l_4=1-\rho^2$, $0<\rho<1$, then $P(\psi)=nc(\psi,\rho)$ and we have

$$q_5\left(x,t\right)=\left[\frac{\lambda\sqrt{1+n}\sqrt{\left(-a+4\beta\right)h_4}}{\sqrt{b}n}\left(\frac{nc(\psi,\rho)}{\sqrt{f\left(nc(\psi,\rho)\right)^2+g}}\right)\right]^{\frac{1}{n}}e^{i(-kx+wt+\theta)}, \tag{4.39}$$

where f and g are given by

$$f=\frac{-(-1+2\rho^2-h_2)h_4}{1-\rho^2+\rho^4-h_2^2},$$
$$g=\frac{3\rho^2h_4}{1-\rho^2+\rho^4-h_2^2},$$

under the constraint condition

$$h_4^2\left(-1+2\rho^2-h_2\right)\left[\left(-2+\rho^2+h_2\right)\left(1+\rho^2+h_2\right)\right]=0.$$

If $\rho\to 1$, then the solitary wave solution is obtained

$$q_{5,1}\left(x,t\right)=\left[\frac{\lambda\sqrt{1+n}\sqrt{\left(-a+4\beta\right)h_4}}{\sqrt{b}n}\left(\frac{\cosh(\psi)}{\sqrt{\frac{(-3+(1-h_2)\cosh^2(\psi))h_4}{-1+h_2^2}}}\right)\right]^{\frac{1}{n}}e^{i(-kx+wt+\theta)}, \tag{4.40}$$

such that

$$h_4^2\left(1-h_2\right)\left[-2+h_2+h_2^2\right]=0.$$

If $\rho\to 0$, then the periodic solution is obtained

$$q_{5,2}\left(x,t\right)=\left[\frac{\lambda\sqrt{1+n}\sqrt{\left(-a+4\beta\right)h_4}}{\sqrt{b}n}\left(\frac{\sec(\psi)}{\sqrt{\frac{-h_4\sec^2(\psi)}{-1+h_2}}}\right)\right]^{\frac{1}{n}}e^{i(-kx+wt+\theta)}, \tag{4.41}$$

such that

$$h_4^2\left(-1-h_2\right)\left[\left(-2+h_2\right)\left(1+h_2\right)\right]=0.$$

6. If $l_0=-1$, $l_2=2-\rho^2$, $l_4=-\left(1-\rho^2\right)$, $0<\rho<1$, then $P(\psi)=nd(\psi,\rho)$ and we have

$$q_6\left(x,t\right)=\left[\frac{\lambda\sqrt{1+n}\sqrt{\left(-a+4\beta\right)h_4}}{\sqrt{b}n}\left(\frac{nd(\psi,\rho)}{\sqrt{f\left(nd(\psi,\rho)\right)^2+g}}\right)\right]^{\frac{1}{n}}e^{i(-kx+wt+\theta)}, \tag{4.42}$$

where f and g are given by

$$f = \frac{(-2+\rho^2+h_2)h_4}{1-\rho^2+\rho^4-h_2^2},$$
$$g = \frac{3h_4}{1-\rho^2+\rho^4-h_2^2},$$

under the constraint condition

$$h_4^2\left(2-\rho^2-h_2\right)\left[-\left(-1+2\rho^2-h_2\right)\left(1+\rho^2+h_2\right)\right]=0.$$

7. If $l_0=1$, $l_2=2-\rho^2$, $l_4=1-\rho^2$, $0<\rho<1$, then $P(\psi)=sc(\psi,\rho)$, and we have

$$q_7(x,t)=\left[\frac{\lambda\sqrt{1+n}\sqrt{(-a+4\beta)\,h_4}}{\sqrt{b}n}\left(\frac{sc(\psi,\rho)}{\sqrt{f\,(sc(\psi,\rho))^2+g}}\right)\right]^{\frac{1}{n}}e^{i(-kx+wt+\theta)}, \tag{4.43}$$

where f and g are given by

$$f = \frac{(-2+\rho^2+h_2)h_4}{1-\rho^2+\rho^4-h_2^2},$$
$$g = \frac{-3h_4}{1-\rho^2+\rho^4-h_2^2},$$

under the constraint condition

$$h_4^2\left(2-\rho^2-h_2\right)\left[-\left(-1+2\rho^2-h_2\right)\left(1+\rho^2+h_2\right)\right]=0.$$

If $\rho\to1$, then the singular soliton solution is obtained

$$q_{7,1}(x,t)=\left[\frac{\lambda\sqrt{1+n}\sqrt{(-a+4\beta)\,h_4}}{\sqrt{b}n}\left(\frac{\sinh(\psi)}{\sqrt{\frac{(3+(1-h_2)\sinh^2(\psi))h_4}{-1+h_2^2}}}\right)\right]^{\frac{1}{n}}e^{i(-kx+wt+\theta)}, \tag{4.44}$$

such that

$$h_4^2\,(1-h_2)\left[-2+h_2+h_2^2\right]=0.$$

If $\rho\to0$, then the periodic wave solution is obtained

$$q_{7,2}(x,t)=\left[\frac{\lambda\sqrt{1+n}\sqrt{(-a+4\beta)\,h_4}}{\sqrt{b}n}\left(\frac{\tan(\psi)}{\sqrt{\frac{(3-(-2+h_2)\tan^2(\psi))h_4}{-1+h_2^2}}}\right)\right]^{\frac{1}{n}}e^{i(-kx+wt+\theta)}, \tag{4.45}$$

such that

$$h_4^2\,(2-h_2)\left[(1+h_2)^2\right]=0.$$

8. If $l_0=1$, $l_2=2\rho^2-1$, $l_4=-\rho^2\left(1-\rho^2\right)$, $0<\rho<1$, then $P(\psi)=sd(\psi,\rho)$ and we have

$$q_8(x,t)=\left[\frac{\lambda\sqrt{1+n}\sqrt{(-a+4\beta)\,h_4}}{\sqrt{b}n}\left(\frac{sd(\psi,\rho)}{\sqrt{f\,(sd(\psi,\rho))^2+g}}\right)\right]^{\frac{1}{n}}e^{i(-kx+wt+\theta)}, \tag{4.46}$$

where f and g are given by

$$f = \frac{(-1+2\rho^2-h_2)h_4}{1-\rho^2+\rho^4-h_2^2},$$
$$g = \frac{-3h_4}{1-\rho^2+\rho^4-h_2^2},$$

under the constraint condition

$$h_4^2\left(-1+2\rho^2-h_2\right)\left[\left(-2+\rho^2+h_2\right)\left(1+\rho^2+h_2\right)\right]=0.$$

9. If $l_0 = 1-\rho^2$, $l_2 = 2-\rho^2$, $l_4 = 1$, $0<\rho<1$, then $P(\psi) = cs(\psi,\rho)$ and we have

$$q_9(x,t) = \left[\frac{\lambda\sqrt{1+n}\sqrt{(-a+4\beta)h_4}}{\sqrt{b}n}\left(\frac{cs(\psi,\rho)}{\sqrt{f\left(cs(\psi,\rho)\right)^2+g}}\right)\right]^{\frac{1}{n}} e^{i(-kx+wt+\theta)}, \tag{4.47}$$

where f and g are given by

$$f = \frac{(-2+\rho^2+h_2)h_4}{1-\rho^2+\rho^4-h_2^2},$$
$$g = \frac{3(-1+\rho^2)h_4}{1-\rho^2+\rho^4-h_2^2},$$

under the constraint condition

$$h_4^2\left(2-\rho^2-h_2\right)\left[-\left(-1+2\rho^2-h_2\right)\left(1+\rho^2+h_2\right)\right]=0.$$

If $\rho\to 1$, then the singular soliton solution is obtained

$$q_{9,1}(x,t) = \left[\frac{\lambda\sqrt{1+n}\sqrt{(-a+4\beta)h_4}}{\sqrt{b}n}\left(\frac{\operatorname{csch}(\psi)}{\sqrt{\frac{-\operatorname{csch}^2(\psi)h_4}{1+h_2}}}\right)\right]^{\frac{1}{n}} e^{i(-kx+wt+\theta)}, \tag{4.48}$$

such that

$$h_4^2(1-h_2)\left[-2+h_2+h_2^2\right]=0.$$

If $\rho\to 0$, then the periodic wave solution is obtained

$$q_{9,2}(x,t) = \left[\frac{\lambda\sqrt{1+n}\sqrt{(-a+4\beta)h_4}}{\sqrt{b}n}\left(\frac{\cot(\psi)}{\sqrt{\frac{(3+(2-h_2)\cot^2(\psi))h_4}{-1+h_2^2}}}\right)\right]^{\frac{1}{n}} e^{i(-kx+wt+\theta)}, \tag{4.49}$$

such that

$$h_4^2(2-h_2)\left[(1+h_2)^2\right]=0.$$

10. If $l_0 = -\rho^2\left(1-\rho^2\right)$, $l_2 = 2\rho^2-1$, $l_4 = 1$, $0<\rho<1$, then $P(\psi) = ds(\psi,\rho)$ and we have

$$q_{10}(x,t) = \left[\frac{\lambda\sqrt{1+n}\sqrt{(-a+4\beta)h_4}}{\sqrt{b}n}\left(\frac{ds(\psi,\rho)}{\sqrt{f\left(ds(\psi,\rho)\right)^2+g}}\right)\right]^{\frac{1}{n}} e^{i(-kx+wt+\theta)}, \tag{4.50}$$

where f and g are given by

$$f = \frac{-(-1+2\rho^2-h_2)h_4}{1-\rho^2+\rho^4-h_2^2},$$
$$g = \frac{-3\rho^2(-1+\rho^2)h_4}{1-\rho^2+\rho^4-h_2^2},$$

under the constraint condition

$$h_4^2\left(-1+2\rho^2-h_2\right)\left[\left(-2+\rho^2+h_2\right)\left(1+\rho^2+h_2\right)\right] = 0.$$

11. If $l_0 = \frac{1-\rho^2}{4}$, $l_2 = \frac{1+\rho^2}{2}$, $l_4 = \frac{1-\rho^2}{4}$, $0 < \rho < 1$, then $P(\psi) = nc(\psi,\rho) \pm sc(\psi,\rho)$ or $P(\psi) = \frac{cn(\psi,\rho)}{1\pm sn(\psi,\rho)}$ and we have

(4.51)
$$q_{11,1}(x,t) = \left[\frac{\lambda\sqrt{1+n}\sqrt{(-a+4\beta)\,h_4}}{\sqrt{b}n}\left(\frac{nc(\psi,\rho)\pm sc(\psi,\rho)}{\sqrt{f\left(nc(\psi,\rho)\pm sc(\psi,\rho)\right)^2+g}}\right)\right]^{\frac{1}{n}} e^{i(-kx+wt+\theta)},$$

or

$$q_{11,2}(x,t) = \left[\frac{\lambda\sqrt{1+n}\sqrt{(-a+4\beta)\,h_4}}{\sqrt{b}n}\left(\frac{\frac{cn(\psi,\rho)}{1\pm sn(\psi,\rho)}}{\sqrt{f\left(\frac{cn(\psi,\rho)}{1\pm sn(\psi,\rho)}\right)^2+g}}\right)\right]^{\frac{1}{n}} e^{i(-kx+wt+\theta)}, \tag{4.52}$$

where f and g are given by

$$f = \frac{-8(1+\rho^2-2h_2)h_4}{1+14\rho^2+\rho^4-16h_2^2},$$
$$g = \frac{12(-1+\rho^2)h_4}{1+14\rho^2+\rho^4-16h_2^2},$$

under the constraint condition

$$h_4^2\left(\frac{1}{2}\left(1+\rho^2-2h_2\right)\right)\left[\frac{1}{16}\left(1+(-6+\rho)\,\rho+4h_2\right)\left(1+\rho\,(6+\rho)+4h_2\right)\right] = 0.$$

If $\rho \to 1$, then the combined singular soliton solution is obtained

$$q_{11,3}(x,t) = \left[\frac{\lambda\sqrt{1+n}\sqrt{(-a+4\beta)\,h_4}}{\sqrt{b}n}\left(\frac{\sinh(\psi)+\cosh(\psi)}{\sqrt{\frac{-h_4(\sinh(\psi)+\cosh(\psi))^2}{1+h_2}}}\right)\right]^{\frac{1}{n}} e^{i(-kx+wt+\theta)}, \tag{4.53}$$

or

$$q_{11,4}(x,t) = \left[\frac{\lambda\sqrt{1+n}\sqrt{(-a+4\beta)\,h_4}}{\sqrt{b}n}\left(\frac{\cosh(\psi)-\sinh(\psi)}{\sqrt{\frac{-h_4(\cosh(\psi)-\sinh(\psi))^2}{1+h_2}}}\right)\right]^{\frac{1}{n}} e^{i(-kx+wt+\theta)}, \tag{4.54}$$

such that

$$h_4^2\,(1-h_2)\left[-2+h_2+h_2^2\right] = 0.$$

If $\rho \to 0$, then the combined periodic wave solutions
(4.55)

$$q_{11,5}(x,t) = \frac{1}{\sqrt{2}}\left[\frac{\lambda\sqrt{1+n}\sqrt{(-a+4\beta)h_4}}{\sqrt{b}n}\left(\frac{\sec(\psi)+\tan(\psi)}{\sqrt{\frac{h_4(-5+4h_2+(1+4h_2)\sin(\psi))}{(-1+\sin(\psi))\left(-1+16h_2^2\right)}}}\right)\right]^{\frac{1}{n}} e^{i(-kx+wt+\theta)},$$

or

$$q_{11,6}(x,t) = \left[\frac{\lambda\sqrt{1+n}\sqrt{(-a+4\beta)h_4}}{2\sqrt{b}n}\left(\frac{\frac{\cos(\psi)}{1+\sin(\psi)}}{\sqrt{\frac{h_4(5-4h_2+(1+4h_2)\sin(\psi))}{(1+\sin(\psi))\left(-1+16h_2^2\right)}}}\right)\right]^{\frac{1}{n}} e^{i(-kx+wt+\theta)}, \tag{4.56}$$

are obtained, such that

$$h_4^2\left(\frac{1}{2}-h_2\right)\left[\frac{1}{16}(1+4h_2)^2\right]=0.$$

12. If $l_0 = \frac{-\left(1-\rho^2\right)^2}{4}$, $l_2 = \frac{1+\rho^2}{2}$, $l_4 = \frac{-1}{4}$, $0<\rho<1$, then $P(\psi) = \rho cn(\psi,\rho) \pm dn(\psi,\rho)$ and we have

(4.57)

$$q_{12}(x,t) = \left[\frac{\lambda\sqrt{1+n}\sqrt{(-a+4\beta)h_4}}{\sqrt{b}n}\left(\frac{\rho cn(\psi,\rho) \pm dn(\psi,\rho)}{\sqrt{f\left(\rho cn(\psi,\rho) \pm dn(\psi,\rho)\right)^2+g}}\right)\right]^{\frac{1}{n}} e^{i(-kx+wt+\theta)},$$

where f and g are given by

$$f = \frac{-8(1+\rho^2-2h_2)h_4}{1+14\rho^2+\rho^4-16h_2^2},$$
$$g = \frac{12(-1+\rho^2)^2h_4}{1+14\rho^2+\rho^4-16h_2^2},$$

under the constraint condition

$$h_4^2\left(\frac{1}{2}\left(1+\rho^2-2h_2\right)\right)\left[\frac{1}{16}\left(1+(-6+\rho)\rho+4h_2\right)\left(1+\rho(6+\rho)+4h_2\right)\right]=0.$$

If $\rho \to 1$, then the singular soliton solution is obtained

$$q_{12,1}(x,t) = \left[\frac{\lambda\sqrt{1+n}\sqrt{(-a+4\beta)h_4}}{\sqrt{b}n}\left(\frac{sech(\psi)}{\sqrt{\frac{-h_4 sech^2(\psi)}{1+h_2}}}\right)\right]^{\frac{1}{n}} e^{i(-kx+wt+\theta)} \tag{4.58}$$

such that

$$h_4^2(1-h_2)\left[-2+h_2+h_2^2\right]=0.$$

If $\rho \to 0$, then the periodic wave solution is obtained

$$q_{12,2}(x,t) = \left[\frac{\lambda\sqrt{1+n}\sqrt{(-a+4\beta)h_4}}{2\sqrt{b}n}\left(\frac{\cos(\psi)}{\sqrt{\frac{h_4(-2+\cos(2\psi)-4h_2\cos^2(\psi))}{-1+16h_2^2}}}\right)\right]^{\frac{1}{n}} e^{i(-kx+wt+\theta)}, \tag{4.59}$$

such that

$$h_4^2\left(\frac{1}{2}-h_2\right)\left[\frac{1}{16}\left(1+4h_2\right)^2\right]=0.$$

13. If $l_0=\frac{1}{4}, l_2=\frac{1-2\rho^2}{2}, l_4=\frac{1}{4}, 0<\rho<1$, then $P(\psi)=\frac{sn(\psi,\rho)}{1\pm cn(\psi,\rho)}$ and we have

$$q_{13}\left(x,t\right)=\left[\frac{\lambda\sqrt{1+n}\sqrt{\left(-a+4\beta\right)h_4}}{\sqrt{b}n}\left(\frac{\frac{sn(\psi,\rho)}{1\pm cn(\psi,\rho)}}{\sqrt{f\left(\frac{sn(\psi,\rho)}{1\pm cn(\psi,\rho)}\right)^2+g}}\right)\right]^{\frac{1}{n}}e^{i(-kx+wt+\theta)}, \tag{4.60}$$

where f and g are given by

$$f=\frac{8(-1+2\rho^2+2h_2)h_4}{1-16\rho^2+16\rho^4-16h_2^2},$$
$$g=\frac{-12h_4}{1-16\rho^2+16\rho^4-16h_2^2},$$

under the constraint condition

$$h_4^2\left(\frac{1}{2}-\rho^2-h_2\right)\left[\frac{1}{16}+2\rho^2-2\rho^4+\left(\frac{1}{2}-\rho^2\right)h_2+h_2^2\right]=0.$$

If $\rho\to 1$, then the combined solitary solution is obtained

$$q_{13,1}\left(x,t\right)=\left[\frac{\lambda\sqrt{1+n}\sqrt{\left(-a+4\beta\right)h_4}}{2\sqrt{b}n}\left(\frac{\tanh(\frac{\psi}{2})}{\sqrt{\frac{h_4(5+(1-4h_2)\cosh(\psi)+4h_2)}{(1+\cosh(\psi))\left(-1+16h_2^2\right)}}}\right)\right]^{\frac{1}{n}}e^{i(-kx+wt+\theta)}, \tag{4.61}$$

such that

$$h_4^2\left(\frac{-1}{2}-h_2\right)\left[\frac{1}{16}\left(1-4h_2\right)^2\right]=0.$$

If $\rho\to 0$, then the combined periodic wave solution is obtained

$$q_{13,2}\left(x,t\right)=\left[\frac{\lambda\sqrt{1+n}\sqrt{\left(-a+4\beta\right)h_4}}{2\sqrt{b}n}\left(\frac{\frac{\sin(\psi)}{1+\cos(\psi)}}{\sqrt{\frac{h_4\left(3+2(1-2h_2)\left(\frac{\sin(\psi)}{1+\cos(\psi)}\right)^2\right)}{\left(-1+16h_2^2\right)}}}\right)\right]^{\frac{1}{n}}e^{i(-kx+wt+\theta)}, \tag{4.62}$$

such that

$$h_4^2\left(\frac{1}{2}-h_2\right)\left[\frac{1}{16}\left(1+4h_2\right)^2\right]=0.$$

Figures 5 and 6 showcase the remarkable duality of nonlinear wave solutions in the φ^6-CGLE system, spanning from singular solitons to periodic waves. Figure 5 captures the singular soliton $q_{13,1}$ ($\rho\to 1$), characterized by a sharp, kink-like intensity dip (panel a) and stable propagation (panel b), arising from the interplay of anomalous dispersion ($a=1$) and focusing nonlinearity ($h_4=-0.82$). This solution models Optical rogue waves or topological defects, with its phase discontinuity offering potential applications in shock wave generation and singular optics. In contrast, Figure 6 displays a periodic solution $q_{13,2}$ ($m\to 0$), where trigonometric modulation (panel a) and coherent wavefronts (panel b) reflect parametric wave mixing or Brillouin scattering in dispersion-managed systems. The transition from singular Figure 5 to periodic Figure 6 states controlled by the elliptic modulus ρ highlights the system's

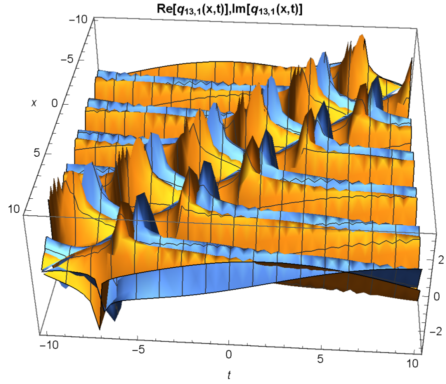

(A) $|q_{13,1}|$

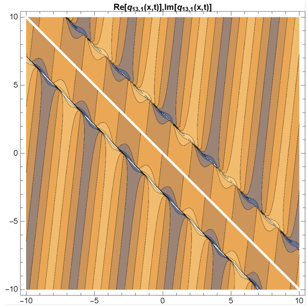

(B) $|q_{13,1}|$

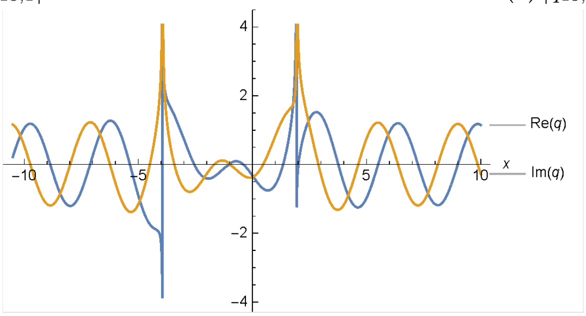

(C) $|q_{13,1}|$

FIGURE 5. The numerical simulations corresponding to $|q_{13,1}|$ given by Eq. (4.61), for $\rho = 1$; (a) is the 3D graphic, (b) is the 2D-contour graphic while (c) is the 3D graphic for $k = 1.8, \theta = 5, \omega = 0.2, v = -1, \gamma = 1, \beta = 0.8, a = 1, n = 1.3, \lambda = 0.6, h_4 = -0.82, c = 1.2, \alpha_1 = 1, h_2 = 1$.

versatility, with h_2 and h_4 tuning amplitude and stability. Together, these figures demonstrate the φ^6-CGLE capacity to support diverse wave phenomena, from localized singularities to extended periodic patterns, paving the way for advanced optical technologies in frequency comb generation, soliton communication, and nonlinear signal processing. This concludes our analysis, underscoring the rich nonlinear dynamics achievable through parameter engineering in higher-order wave systems.

14. If $l_0 = \frac{1}{4}, l_2 = \frac{1+\rho^2}{2}, l_4 = \frac{(1-\rho^2)^2}{4}, 0 < \rho < 1$, then $P(\psi) = \frac{sn(\psi,\rho)}{cn(\psi,\rho) \pm dn(\psi,\rho)}$ and we have

$$q_{14}(x,t) = \left[\frac{\lambda\sqrt{1+n}\sqrt{(-a+4\beta)\,h_4}}{\sqrt{b}n} \left(\frac{\frac{sn(\psi,\rho)}{cn(\psi,\rho)\pm dn(\psi,\rho)}}{\sqrt{f\left(\frac{sn(\psi,\rho)}{cn(\psi,\rho)\pm dn(\psi,\rho)}\right)^2 + g}} \right) \right]^{\frac{1}{n}} e^{i(-kx+wt+\theta)}, \tag{4.63}$$

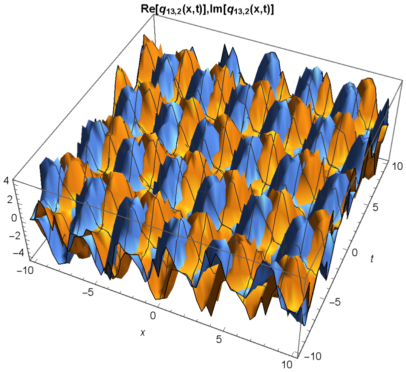

(A) $|q_{13,2}|$

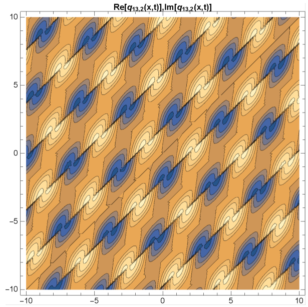

(B) $|q_{13,2}|$

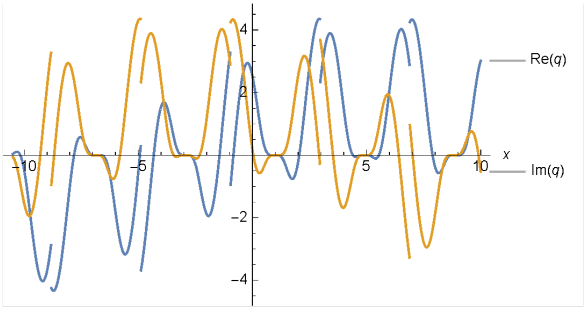

(C) $|q_{13,2}|$

FIGURE 6. The numerical simulations corresponding to $|q_{13,2}|$ given by Eq. (4.62), for $\rho = 0$; (a) is the 3D graphic, (b) is the 2D-contour graphic while (c) is the 3D graphic for $k = 1.8, \theta = 5, \omega = 0.26, v = 1, \gamma = 1, \beta = 0.8, a = 1, n = 0.23, \lambda = 1.6, h_4 = 0.8, c = 1.2, \alpha_1 = 1, h_2 = -2$.

where f and g are given by

$$f = \frac{-8(1+\rho^2-2h_2)h_4}{1+14\rho^2+\rho^4-16h_2^2},$$
$$g = \frac{-12h_4}{1+14\rho^2+\rho^4-16h_2^2},$$

under the constraint condition

$$h_4^2\left(\frac{1}{2}\left(1+\rho^2-2h_2\right)\right)\left[\frac{1}{16}\left(1+\left(-6+\rho\right)\rho+4h_2\right)\left(1+\rho\left(6+\rho\right)+4h_2\right)\right]=0.$$

If $\rho \to 1$, then the singular soliton solution is obtained

$$q_{14,1}\left(x,t\right) = \left[\frac{\lambda\sqrt{1+n}\sqrt{\left(-a+4\beta\right)h_4}}{\sqrt{b}n}\left(\frac{\sinh(\psi)}{\sqrt{\frac{h_4(3+(1-h_2)\sinh^2(\psi))}{-1+h_2^2}}}\right)\right]^{\frac{1}{n}} e^{i(-kx+wt+\theta)}, \tag{4.64}$$

such that

$$h_4^2\left(1-h_2\right)\left[-2+h_2+h_2^2\right]=0.$$

If $\rho \to 0$, then the periodic wave is obtained

$$(4.65)\quad q_{14,2}\left(x,t\right)=\left[\frac{\lambda\sqrt{1+n}\sqrt{\left(-a+4\beta\right)h_{4}}}{2\sqrt{b}n}\left(\frac{\frac{\sin(\psi)}{1+\cos(\psi)}}{\sqrt{\frac{h_{4}\left(3+2(1-2h_{2})\left(\frac{\sin(\psi)}{1+\cos(\psi)}\right)^{2}\right)}{-1+16h_{2}^{2}}}}\right)\right]^{\frac{1}{n}}e^{i(-kx+wt+\theta)},$$

such that

$$h_{4}^{2}\left(\frac{1}{2}-h_{2}\right)\left[\frac{1}{16}\left(1+4h_{2}\right)^{2}\right]=0.$$

5. Remarks

This study examines the Complex GinzburgLandau Equation (CGLE) for soliton propagation in nonlinear optics, accounting for the presence of a detuning factor. By applying the φ^6-model expansion method, explicit solutions for bright, dark, periodic, and darkbright solitons are obtained, along with singular soliton solutions. The analysis is conducted within the framework of power-law nonlinear fibers. The findings are expected to enhance understanding of the nonlinear dynamical properties of the CGLE. The proposed method offers an efficient and practical approach for deriving exact solutions to a broad class of nonlinear fractional partial differential equations.

Figures 1–3 illustrate the temporal behavior of dark, bright, darkbright, periodic, and combined periodic wave solutions, which are relevant to the transmission of energy between spatial locations. Additionally, the study explores the physical interpretation of the parameters involved in the classical wave transformation, described by Eqs. (2.1) and (2.2). The solutions to Eqs. (4.26), (4.28), (4.30), (4.31), (4.61), and (4.62) describe traveling waves that incorporate various mathematical constants, reflecting the internal dynamics of the wave under different parameter values. It is observed that variations in these parameters lead to notable changes in the traveling wave behavior. In particular, the discussion highlights how changes in the soliton frequency k influence one of the key internal dynamics of the traveling wave.

6. Conclusion

In this study, we have investigated the propagation of optical solitons in nonlinear fibers governed by the Complex GinzburgLandau Equation (CGLE) with power-law nonlinearity, incorporating the physical effect of detuning. By employing the recently developed φ^6model expansion method, we have successfully derived a rich variety of exact traveling wave solutions, including bright solitons, dark solitons, singular solitons, periodic waves, and several hybrid structures such as darkbright and combined singular forms. The method demonstrated remarkable efficiency and flexibility in handling the nonlinear structure of the CGLE, yielding solutions expressed in terms of Jacobi elliptic functions, hyperbolic, trigonometric, rational, and mixed functional forms. In the limiting cases where the modulus $\rho \to 1$ or $\rho \to 0$, these general solutions reduce to well-known localized solitons or periodic wave patterns, confirming their physical consistency and dynamical relevance. In particular, the emergence of both bright and dark solitons under appropriate parametric conditions highlights the model's ability to describe diverse nonlinear wave phenomena in optical media with power-law dependence.

From a physical standpoint, the derived solutions contribute meaningfully to the understanding of non-linear wave dynamics in optical fibers with power-law non-linearity, a generalization of the standard Kerr law that applies to a wide range of real-world materials, including semiconductors and doped fibers. These findings have direct implications for modern optical communication technologies, including ultra-fast pulse transmission, all-optical switching, signal encoding, and the management of intensity dips and phase discontinuities in logic-based photonic circuits.

In summary, this research not only advances the analytical treatment of the CGLE under power-law nonlinearity but also opens new possibilities for engineering stable and controllable solitonic structures in nonlinear fiber optics. The interplay between nonlinearity, dispersion, and detuning, as captured by the model, reveals a rich landscape of wave behaviors that can be tuned through parameter engineering. Future studies may extend this framework to coupled systems, birefringent fibers, or fractional-order generalizations, further expanding its applicability in both theoretical and applied photonics.

References

[1] K. S. Al-Ghafri: *Soliton behaviours for the conformable space–time fractional complex Ginzburg–Landau equation in optical fibers,* Symmetry, **12** (2) (2020), Article ID: 219.

[2] A. H. Arnous, A. R. Seadawy, R. T. Alqahtani and A. Biswas: *Optical solitons with complex Ginzburg–Landau equation by modified simple equation method,* Optik, **144** (2017), 475–480.

[3] S. Arshed: *Soliton solutions of fractional complex Ginzburg–Landau equation with Kerr law and non-Kerr law media,* Optik, **160** (2018), 322–332.

[4] A. Biswas, R. T. Alqahtani: *Optical soliton perturbation with complex Ginzburg-Landau equation by semi-inverse variational principle*. Optik, **147** (2017), 77–81.

[5] B. Ghanbari, D. Baleanu: *A novel technique to construct exact solutions for nonlinear partial differential equations* , Eur. Phys. J. Plus, **134** (10) (2019), Article ID: 506.

[6] A. Hasegawa: *Optical solitons in fibers*. Optical solitons in fibers. Springer, Berlin, Heidelberg (1989).

[7] A. Hasegawa, Y. Kodama: *Signal transmission by optical solitons in monomode fiber,* Proceedings of the IEEE, **69** (9) (1981), 1145–1150.

[8] A. Hijaz, T. A. Khan, H. Durur, G. M. Ismail and A. Yokus: *Analytic approximate solutions of diffusion equations arising in oil pollution,* J. Ocean Eng. Sci., **6** (1), (2021), 62–69.

[9] D. Kaya, A. Yokus and U. Demiroglu: *Comparison of exact and numerical solutions for the Sharma–Tasso–Olver equation,* Num. Sol. Real. Nonlinear Phenomena, Springer, Cham, (2020), 53–65.

[10] C. Keşan: *Taylor polynomial solutions of linear differential equations,* Appl. Math. Comp., **142** (1) (2003), 155–165.

[11] Y. S. Kivshar, G. P. Agrawal: *Optical solitons: from fibers to photonic crystals,* Academic press (2003).

[12] M. A. Isah, A. Yokus and D. Kaya: *Bilinear neural network method for obtaining the exact analytical solutions to nonlinear evolution equations and its application to KdV equation*, Khayyam J. Math., **10** (2), 2024, 228–248.

[13] M. A. Isah, A. Yokus and I. Isah: *Dark lump collision phenomena to a nonlinear evolution model in harmonic crystals." Partial Differ. Equ. Appl. Math.*, (2025), Article ID: 101214.

[14] M. A. Isah, A. Yokus: *Analysis of dynamics of fusion solitons of the generalized* $(3+1)$ *KadomtsevPetviashvili equation*, J. Mahani Math. Res., **13** (2) (2024), 505–533.

[15] M. A. Isah, A. Yokus: *The investigation of several soliton solutions to the complex Ginzburg-Landau model with Kerr law nonlinearity,* Math. Model. Num. Simul. Appl., **2** (3) (2022), 147–163.

[16] M. A. Isah, A. Yokus: *Nonlinear Dispersion Dynamics of Optical Solitons of Zoomeron Equation with New* φ^6*-Model Expansion Approach*, J. Vib. Test. Syst. Dyn., **8** (3) (2024), 285–307.

[17] M. A. Isah, A. Yokus: *A novel technique to construct exact solutions for the Complex Ginzburg-Landau equation using quadratic-cubic nonlinearity law,* Math. Eng., Sci. & Aer. (MESA), **14** (1) (2023).

[18] I. Isah, M. A. Isah, M. U. Baba, T. L. Hassan and K. D. Kabir: *On integrability of silver Riemannian structure,* Int. J. Adv. Aca. Res., **7** (12) (2021), 2488–9849.

[19] W. Malfliet: *Solitary wave solutions of nonlinear wave equations*, Am. J. Phys., **60** (7) (1992), 650–654.

[20] A. Muhammad, I. A. Auwal, A. Abdullahi and M. A. Isah: *Alpha and beta radioactivity concentration assessments in drinking water along the Kumbotso pipeline, Kano*, Avicenna, **2** (2025), Article ID: 10.

[21] Z. H. Musslimani, K. G. Makris, R. El-Ganainy and D. N. Christodoulides: *Optical solitons in P T periodic potentials,* Phys. Rev. Let., **100** (3) (2008), Article ID: 030402.

[22] D. Serbay, A. Yokus, H. Durur and D. Kaya: *Refraction simulation of internal solitary waves for the fractional Benjamin–Ono equation in fluid dynamics,* Modern Phys. Let. B, (2021), Article ID: 2150363.

[23] T. Ueda, W. L. Kath: *Dynamics of coupled solitons in nonlinear optical fibers,* Phys. Rev. A, **42** (1) (1990), Article ID: 563.

[24] A. Yokus, H. Durur, K. A. Abro and D. Kaya: *Role of Gilson–Pickering equation for the different types of soliton solutions: a nonlinear analysis,* Eur. Phys. J. Plus, **135** (8) (2020), 1–19.

[25] A. Yokus, M. A. Isah: *Stability analysis and solutions of* $(2+1)-$*KadomtsevPetviashvili equation by homoclinic technique based on Hirota bilinear form*. Nonlinear Dyn., **109** (2022), 3029–3040.

[26] A. Yokus, M. A. Isah and M. Tuz: *Analytical Investigation of Nonlinear Distribution Mechanisms in Fluid Dynamics through the Boiti-Leon-Manna-Pempinelli Equation,* Comp. Math. Model., (2025), 1–16.

[27] A. Yokus, M. A. Isah: *Unveiling novel insights: Nonlinear dispersion dynamics of optical solitons through new* φ^6*-Model expansion in the KleinGordon equation,* Chinese J. Phys., **95** (2025), 476–492.

[28] E. M. E. Zayed, M. E. M. Alngar, M. El-Horbaty, A. Biswas, A. S. Alshomrani, M. Ekici, Y. Yldrm, M. R. Belic: *Optical solitons with complex Ginzburg–Landau equation,* Nonlinear Dyn., **85** (3) (2016), 1979–2016.

[29] E. M. E. Zayed, A. G. Al-Nowehy and M. E. Elshater: *New* φ^6*-model expansion method and its applications to the resonant nonlinear Schrödinger equation with parabolic law nonlinearity,* Eur. Phys. J. Plus, **133** (2018): Article ID: 417.

Muhammad Abubakar Isah
Istanbul Ticaret University
Department of Mathematics
34445, Istanbul, Türkiye
Email address: myphysics_09@hotmail.com

Ahmad Muhammad
Qatar University
Department of Physics and Materials Sciences
Doha, 2713, Qatar
Email address: a.muhammad@qu.edu.qa